Nationaal Lucht- en Ruimtevaartlaboratorium

National Aerospace Laboratory NLR

NLR-TP-99392

Significance of dwell cracking for IN718 turbine discs

R.J.H. Wanhill

Nationaal Lucht- en Ruimtevaartlaboratorium
National Aerospace Laboratory NLR

NLR-TP-99392

Significance of dwell cracking for IN718 turbine discs

R.J.H. Wanhill

This report is based on an article to be published in a special issue of the International Journal of Fatigue.

Division: Structures and Materials
Issued: September 1999
Classification of title: Unclassified

Contents

(29 pages in total)

This page is intentionally left blank.

SIGNIFICANCE OF DWELL CRACKING FOR IN718 TURBINE DISCS

R.J.H. Wanhill
National Aerospace Laboratory NLR, P.O. Box 153, 8300 AD Emmeloord, The Netherlands

High temperature “dwell cracking” of the nickel-base superalloy IN718 was investigated as part of a European project on military aircraft turbine discs. Dwell and fatigue crack growths tests under simple loading conditions indicated that dwell cracking would be unlikely to occur under actual flight loadings and that standard fracture mechanics specimens may be inappropriate for predicting crack growth in discs. Flight-by-flight loading tests showed that dwell cracking was either absent or limited.

(Keywords: superalloys; high temperature crack growth)

INTRODUCTION

From 1989 to 1997 a European cooperative technology project was done with the title “Lifing Concepts for Military Aero-Engine Components” [1]. The participants were two engine manufacturers, EGT –now ALSTOM (UK) and MTU (GE), and four research institutes, IABG and RWTH (GE), DERA (UK) and the NLR (NL). The main objectives of the project were:

(1) Examination of existing disc lifing methodologies applied to highly stressed components operating at high temperatures.
(2) To ascertain whether a better understanding of low cycle fatigue (LCF) and crack growth mechanisms at high stresses and temperatures could lead to improved lifing methodologies.

The present paper is a contribution to objective (2) and is concerned with determining the usefulness of developing crack growth prediction methods that combine dwell or creep crack growth (not necessarily the same phenomenon, as will be shown) with fatigue crack growth. The following aspects of dwell and fatigue cracking were investigated: fracture mechanics characterizations of dwell crack growth; effects of peak loads and underloads on dwell crack growth; fatigue crack growth + dwells in standard and engineering specimens; and crack growth under flight-by flight loading, all at 600 °C.

MATERIAL AND SPECIMENS

The material was a batch of 440 mm diameter x 66 mm thick forged pancakes of IN718 manufactured by SNECMA (FR). Table 1 gives the material heat treatment, mechanical properties and grain size. The heat treatment is a well-established one for obtaining optimum creep resistance.

The main specimen type used for crack growth tests was the standard compact tension (CT) configuration shown in figure 1. The other specimen types, namely LCF, cornercrack (CC) and the engineering rim (RIM) specimens, are shown in figures 2-4. The orientations and locations of the specimens were chosen to reflect any directionality in the pancake forgings and also to avoid the central “dead zone” of minimum working [4].

TEST PROGRAMME

Table 2 gives an overview of the test programme, which was done with specimens in an air environment of 0.1 MPa (1 atm) at 600 °C. There are three main sub-divisions:

(1) Dwell cracking and effects of peak loads and underloads.

(2) Behaviour of standard (CT) and engineering (RIM) specimens under fatigue crack growth + dwells.

(3) Behaviour under flight-by-flight loading (HOT TURBISTAN).

At this point the main items for clarification of table 2 are the non-standard fatigue load histories. The trapezoidal waveforms consisted of 1s minimum loads and upward and downward ramp loadings, with in-between dwells of 1s and 120s at maximum load. The flight-by-flight loading sequence HOT TURBISTAN is fully described in Ref. [5]. Figure 5 shows a typical segment of the HOT TURBISTAN sequence, which is an isothermalised generic load history for military aircraft turbine discs, with all dwells below the peak loads. The sequence consists of repeated blocks of 100 different flights containing 689 dwell periods varying from 1s to 798s. The accumulated dwell time per 100 flights is 8hr 27s.

DWELL CRACKING AND EFFECTS OF PEAK LOADS AND UNDERLOADS

Experimental procedure

The CT specimens were fatigue pre-cracked under constant amplitude loading, R=0.1, with maximum loads P_{max} between 6 and 8 kN. The fatigue pre-cracks were grown to between 2 and 4 mm from the notch root. Seven specimens were subjected to dwell testing, i.e. constant load crack growth tests, and three specimens were subjected to dwell tests with peak loads and underloads as shown in table 2. The peak loads were immediately followed by underloads, as is often the case for military aircraft turbine discs. Furthermore, the immediate succession of peak loads by underloads is conservative, since this is most likely to minimise any retarding or inhibiting effect of peak loads on subsequent dwell crack growth.

The experimental details are given fully in Refs. [6-8]. Here it is important to note that the CT specimen crack lengths were measured with the direct current potential drop (PD) method, whereby the specimens were insulated from the load frame by a 0.3 mm thick $Al_2 0_3$ ceramic coating on the loading pins; and a reference voltage was obtained from a companion specimen inside the furnace. Also, the crack opening displacements at the load line (pin centre-to-centre) were measured with linear variable displacement transducers (LVDTs).

Fracture mechanics characterizations of dwell growth: results

A full description of this part of the programme is given in Ref. [6]. Here follows an extended summary of the results. The PD and LVDT data were processed to obtain the following:

(1) Correlations between dwell crack growth and crack growth rates, da/dt, and the fracture mechanics parameters K_I , J and C*. Determination of K_I is straightforward, using the standard CT expression [9]. However, J and C* may be determined by several methods, and in the present work was done in two ways. First the experiment-based procedure developed by Kumar *et al* [10] was used as the main method of determining J and C*. This method requires, among other quantities, the value of the exponent n in the Norton creep law $\dot{\varepsilon} = A\sigma^n$. Secondly, selected values of J and C* were obtained by finite element analysis using MARC and a post-processor program [11]. This method requires the values of both A and n in the Norton creep law.

(2) Comparisons between the experimental and analytical load-line compliances.

(3) Values of the characteristic time, t_c , for distinguishing between small-scale yielding and extensive creep. An analytical expression for t_c is [12]:

$$t_c = K_I^2 \left(1-\nu^2\right) \Big/ \left[(n+1)\, EC^* \right] \tag{1}$$

where ν and E are Poisson’s ratio and Young’s modulus, respectively. Provided the actual deformation behaviour of a specimen is governed by creep, then comparison of experimentally derived values of t_c (using C* values derived by the method of Kumar *et al* [10]) with the actual testing time, t , should show $t_c >> t$ for small-scale yielding and $t_c << t$ for extensive creep.

The dwell crack growth rates were well correlated by K_I and experimentally-derived values of J and C* *per se* [6]. However, more importantly the experimental and analytical values for both J and C* were very different. In particular, the differences between C* values were enormous, as figure 6 illustrates in a plot of dwell crack length, a , versus C*.

Figure 7 compares the experimental load-line compliances with the analytical elastic solution [13]. The general trend of the experimental data is to follow the analytical curve, as found by others for IN718 tested in air at 650 °C [14]. In other words, the compliance data indicate that elastic deformation predominates during dwell crack growth at temperatures up to 650 °C.

Figure 8 compares the dwell crack growth lives with the characteristic times, t_c. Since $t_c << t$, figure 8 indicates that if the actual deformation behaviour of the specimens were to be governed by creep, then extensive creep should have occurred. However, this is incompatible with the load-line compliance measurements, figure 7.

Fracture mechanics characterizations of dwell crack growth: discussion

The foregoing results can be explained only if dwell cracking is not governed by creep (specifically, power-law creep) but by a nominally elastic crack growth process. In fact, there is much evidence that dwell cracking in nickel-base superalloys is a stress-assisted process of grain boundary oxidation and subsequent intergranular fracture [15-17] involving only highly localised and inhomogeneous plasticity. The fractographic results for the CT specimens [6] were consistent with this evidence.

There are two important points that follow from this explanation. Firstly, a nominally elastic crack growth process explains why K_I provides good correlations of crack growth rates and also correlates data from different investigations in a consistent manner, figure 9. Secondly, it is known that oxidation-controlled dwell cracking is hindered by prestraining that results in (local) homogeneous plastic deformation in IN718 [16,19].

Effects of peak loads and underloads on dwell crack growth

Peak loads strongly inhibited dwell cracking even when immediately followed by underloads [6]. An example is given in figure 10. The suppression of dwell cracking lasted for several hours, which is much longer than dwell periods for military aircraft turbine discs. Suppression of dwell cracking was also obtained in another part of this European project, where repetitive load histories similar to the single load history in figure 10 were applied [1, 20].

An explanation for the strong inhibition of dwell cracking by peak loads involves a chain of evidence. Firstly, the balance of evidence from previous work [14-17] and the present investigation leads to the conclusion that dwell crack growth in IN718 occurs under small-scale yielding conditions at temperatures up to 650 °C, and is environmentally controlled and takes place by grain boundary oxidation and subsequent intergranular fracture, as mentioned above. Creep deformation in the crack tip region must be limited, if any, and must generally occur at a much slower rate, as shown by comparisons of dwell crack growth tests in air and inert environments (presumably only creep crack growth) [21,22]. Secondly, under small-scale yielding a peak load, even if immediately followed by an underload, would be expected to result in residual compressive stresses at - or very close to – the crack tip. These compressive stresses would be only very slowly relaxed by creep and would therefore hinder the fracture of oxidised grain boundaries. Thirdly, the peak load locally prestrains the material at the crack tip, thereby hindering the process of grain boundary oxidation [19].

CT AND ENGINEERING (RIM) SPECIMEN FATIGUE CRACK GROWTH + DWELLS

The middle part of table 2 gives an overview of the test programme, which is described in Refs. [23,24]. The CT specimens represented standard crack growth testing from a pre-cracked configuration. However, the RIM specimens, whose notches generically simulate blade slots at the rim of a turbine disc, did not have crack starters. The RIM specimen tests were basically LCF, with marker cycles added for eventual “readability” of the fracture surfaces for determination of crack growth. The RIM specimen load histories were repeated blocks of 1000 major cycles, R=0.1, alternating with 1000 marker cycles, R=0.8, with the same maximum stress. The insertion of blocks of marker cycles had previously been shown to have no observable effect on the major cycle crack growth rates, and to contribute less than 10 % to the overall crack growth [25].

Determination of RIM specimen fatigue crack growth rates and stress intensity factors

This part of the programme is fully described in Ref. [26]. The RIM specimen fatigue crack growth rates, crack growth lives and hence fatigue initiation lives were determined by the NLR, using the fractography-based method schematically given in figure 11. Stress intensity factors for the natural semi-elliptical cracks growing from the notch surfaces of the RIM specimens were calculated using equations 52-55 and 59-67 in Appendix A of Herbel *et al* [27].

CT and RIM specimen crack growth rates: results and discussion

Figure 12 shows the results. There was a large dwell effect for the CT specimens, similar to that observed for CC specimens [1]. However, this dwell effect was initially absent for the RIM specimens, with the fractographically-obtained data lying in a narrow band superimposed on the CT specimen 2Hz data. The RIM specimen tested with 120s dwells did eventually show dwell cracking, which began at a crack depth of about 1 mm ($\Delta K \sim 50$ MPa$\sqrt{\text{m}}$) and disrupted the fractographic determination of crack growth rates.

There are two possible explanations of the initial absence of dwell effects for the RIM specimens. Firstly, there might have been local mean stress relaxation within the initial plastic zones of the notches, whereby any dwell cracking contributions would be counterbalanced by lower mean stresses and lower effective crack tip loadings. Against this argument are the absence of dwell cracking characteristics (intergranular crack growth) except later on for the RIM specimen tested with 120s dwells, and the virtual coincidence of *all* the RIM specimen data with the CT specimen 2 Hz data.

Secondly, the RIM specimens would most probably have undergone extensive monotonic yielding of the notch roots during the first ¼ cycle, followed by nominally elastic behaviour under subsequent fatigue loads: this is inferred from the behaviour of LCF specimens tested under load control with σ_{max} = 1100 MPa and R=0 [27]. (In fact, for σ_{max} = 750 MPa the depth of monotonic yielding for the RIM specimens was estimated by the author to be between 0.5 – 1 mm, making use of FEM analysis results by Hughes [29].) The initial yielding would then have acted as a prestrain, hindering dwell cracking as discussed earlier.

CRACK GROWTH UNDER FLIGHT-BY-FLIGHT LOADING

The lower part of table 2 gives an overview of the tests with HOT TURBISTAN. Full descriptions of the tests are given in Refs. [1,30,31]. The LCF specimen tests were strain controlled, while the CC and RIM specimen crack growth tests were load controlled. The CC specimens each had one crack starter notch at a corner. The RIM specimens each had two crack starter notches at diametrically opposite corners. However, all three RIM specimens showed crack growth only from one of the crack starter notches.

Examination of LCF specimens

Fractographic examination of the three strain controlled LCF specimens tested by the IABG showed no evidence of dwell cracking that could have occurred during the HOT TURBISTAN dwell periods. The crack propagation mode was almost entirely transgranular and characterized by flattened and smeared fatigue striations [32].

CC and RIM specimens: stress intensity factors, crack growth rates, fractographic characteristics

Stress intensity factors for the CC specimens were calculated using formulae in Appendix A of Ref. [7]. Stress intensity factors for single quarter-elliptical cracks growing from the notch corners of the RIM specimens were calculated using Newman's approximation for symmetrical corner cracks at a hole [33] and a correction factor derived from the difference between one- and two-crack 2D solutions for the RIM specimen, given in figure 20 of Ref. [27].

Figure 13 shows the HOT TURBISTAN 600 °C crack growth rate data for the CC and RIM specimens, together with COLD TURBISTAN 400 °C data for CC specimens. The reason for including the COLD TURBISTAN data is that there are no dwells in this flight-by-flight loading sequence [34]. From figure 13 it is seen that the HOT TURBISTAN data lie above the COLD TURBISTAN data by factors of 2-3 (CC specimens) and 3-4 (RIM versus CC specimens). Much, or all, of the difference for CC specimens could be due solely to the higher temperature facilitating fatigue crack growth *per se*. However, with respect to HOT TURBISTAN the RIM specimen data lie above the CC specimen data by factors of 2-3, and fractographic examination showed mixed transgranular and intergranular fracture for the RIM specimens [30]. Thus it would appear that dwell cracking occurred in the RIM specimens, leading to higher overall crack growth rates, although the effect was not so large as that found for CT specimens tested with dwells at maximum load, see figure 12.

CONCLUDING REMARKS

From the dwell cracking tests and analysis, and also evidence in the literature [14-17, 19-22] it may be concluded that at temperatures up to 650 °C dwell cracking occurs under small-scale yielding conditions (i.e. it is not due to creep), is environmentally controlled and takes place by grain boundary oxidation and subsequent intergranular fracture.

This mechanism has been used to explain the strong inhibition of dwell cracking by peak loads or prestrains: the latter refer to the difference between CT and RIM specimen crack growth rates, figure 12, in a situation where the RIM specimens were allowed to develop natural cracks from the notch roots.

On the other hand, dwell cracking was not completely suppressed in RIM specimens tested under fatigue + dwell at maximum load and HOT TURBISTAN, which simulates flight-by-flight loading in military aircraft turbine discs. Thus the question arises as to the significance of dwell cracking for military aircraft turbine discs in service. There are three aspects to this question:

(1) Evidence from laboratory testing (this paper) and crack growth predictions [1].

(2) Service-related factors extraneous to laboratory testing [6].

(3) Possible generic behaviour of nickel-base superalloys [35].

The test data indicate that the contribution of dwell cracking should be negligible or limited to the later stages of crack growth away from the notches at disc rims. Consistent with this viewpoint, Heuler and Bergmann [1] showed that crack growth predictions which took no account of dwell cracking were quite successful. However, they cautioned that this success should be regarded as fortuitous at present, and that there is a need for more detailed insight, in particular concerning the dependence of dwell cracking on load sequence effects.

Conceivably the only service-related factor that is extraneous to standard laboratory testing is the environmental air pressure of the turbine discs. Cooling air tapped from the compressor is initially at pressures up to about 2.5 MPa (25 atm) in modern military aircraft gas turbines, and since dwell cracking is environmentally controlled it might be thought that such high air pressures could affect the dwell crack growth rates. However, experiments have shown that provided the oxygen partial pressure is above 10 Pa (10^{-4} atm) the kinetics of dwell crack growth are unaffected [15,35]. Thus there is no reason to expect any difference between dwell crack growth rates in service and under standard laboratory testing in air of 0.1 MPa (1 atm).

Finally, although the test data from the present European cooperation technology project are confined to IN718, it is evident from other work that similar dwell crack growth behaviour can occur in more advanced nickel-base superalloys [35]. Thus the present project results would appear to have generic implications for these materials.

ACKNOWLEDGEMENTS

Especial thanks go to the programme coordinators, Paul Heuler and Joachim Bergmann, and to our many international colleagues. The author is grateful for continuing support from many NLR colleagues, notably Jos Boogers, Henk Kolkman, Anne Oldersma and Henk-Jan ten Hoeve, and the Netherlands national coordinators, Frank Beuskens and Charles Hofman. This research was sponsored by the Netherlands Ministry of Defence in liaison with the Netherlands Agency for Aerospace Programmes (NIVR).

REFERENCES

1. Heuler, P. and Bergmann, J.W., A research programme into lifing concepts for military aero-engine components, Industrieanlagen - Betriebsgesellschaft (IABG) Report No. B-TA-3602, Ottobrunn, Germany, August 1997.
2. Honnorat, Y., SNECMA letter YKOM1 No. 68772, Societé Nationale d’Étude et de Construction de Moteurs d’Aviation (SNECMA), Evry, France, May 1989.
3. Wanhill, R.J.H., NLR’s contribution to specimen manufacture for the IEPG TA 31 programme, Memorandum SM-94-021, National Aerospace Laboratory NLR, Amsterdam, The Netherlands, March 1994.
4. Barnard, P.M., Cut up report of Inconel 718 discs supplied by S.N.E.C.M.A. for the TA 31 programme, Report 94-LAB-054, European Gas Turbines, Lincoln, UK, March 1994.
5. Bergmann, J.W. and Schütz, W., Standardised load sequence for turbine and hot compressor discs of combat aircraft engines, Industrieanlagen-Betriebsgesellschaft (IABG) Report TF-2809 (in German), Ottobrunn, Germany, 1990.
6. Wanhill, R.J.H. and Boogers, J.A.M., The effects of peak loads and underloads on dwell crack growth in Inconel 718 at 600 °C – Contribution to IEPG TA 31: lifing concepts for military aero-engine components, NLR Technical Publication TP 93300 L, National Aerospace Laboratory NLR, Amsterdam, The Netherlands, July 1993.
7. Mom, A.J.A. and Raizenne, M.D., AGARD engine disc cooperative test programme, AGARD Report No. 766, Advisory Group for Aerospace Research and Development, Neuilly-sur-Seine, France, August 1988.
8. Van Leeuwen, H.P., Groep, F.F., Schra, L. and Dam, N., Automated measurement of crack length and load line displacement at elevated temperature, AGARD Report No. 751, Advisory Group for Aerospace Research and Development, Neuilly-sur-Seine, France, February 1988.

9. Standard test method for plane-strain fracture toughness of metallic materials, ASTM Standard E399-83, American Society for Testing and Materials 1990 Annual Book of ASTM Standards Section 3: Metals Test Methods and Analytical Procedures, Vol. 03.01, pp. 488-512, Philadelphia, USA, 1990.
10. Kumar, V., German, M.D. and Shih, C.F., An engineering approach for elastic-plastic fracture analysis, EPRI Report NP-1931, Electric Power Research Institute, Palo Alto, USA, July 1981.
11. Bakker, A., Virtual crack extension (VCE) post processor input description, Version 2.3, Delft University of Technology, Delft, The Netherlands, October 1991.
12. Riedel, H. and Rice, J.R., Tensile cracks in creeping solids, Fracture Mechanics: Twelfth Conference, ASTM STP 700, American Society for Testing and Materials, pp. 112-130, Philadelphia, USA, 1980.
13. Saxena, A. and Hudak, S.J., Review and extension of compliance information for common crack growth specimens, International Journal of Fracture, Vol. 14, pp. 453-468, 1978.
14. Liu, C.D., Han, Y.F. and Yan, M.G., Small-scale creep crack growth. Engineering Fracture Mechanics, Vol. 41, pp. 229-239, 1992.
15. Andrieu, E., Ghonem, H. and Pineau, A., Two-stage crack tip oxidation mechanism in alloy 718, Elevated Temperature Crack Growth, MD-Vol.18, The American Society of Mechanical Engineers, pp. 25-29, New York, USA, 1990.
16. Ghonem, H., Nicholas, T. and Pineau, A., Analysis of elevated temperature fatigue crack growth mechanisms in alloy 718, Creep-Fatigue Interaction at High Temperature, AD-Vol. 21, The American Society of Mechanical Engineers, pp. 1-18, New York, USA, 1991.
17. Gao, M., Chen, S.-F., Chen, G.S. and Wei, R.P., Environmentally enhanced crack growth in nickel-based alloys at elevated temperatures, Elevated Temperature Effects on Fatigue and Fracture, ASTM STP 1297, American Society for Testing and Materials, pp. 74-84, West Conshohocken, USA, 1997.
18. Sadananda, K. and Shahinian, P., Creep crack growth in alloy 718, Metallurgical Transactions A, Vol. 8A, pp. 439-449, 1977.
19. Zheng, D., Rosenberger, A. and Ghonem, H., Influence of prestraining on high temperature, low frequency fatigue crack growth in superalloys, Materials Science and Engineering, Vol. A161, pp. 13-21, 1993.
20. Wanhill, R.J.H., Fractographic and metallographic examination of IABG corner crack (CC) specimens, NLR Contract Report CR 96759, National Aerospace Laboratory NLR, Amsterdam, The Netherlands, December 1996.
21. Floreen, S. and Kane, R.H., An investigation of the creep-fatigue-environment interaction in a Ni-base superalloy, Fatigue of Engineering Materials and Structures, Vol. 2, pp. 401-412, 1980.

22. Sadananda, K., and Shaninian, P., The effect of environment on the creep crack growth behaviour of several structural alloys, Materials Science and Engineering, Vol. 43, pp. 159-168, 1980.
23. Barnard, P., Notched disc specimen testing, IEPG TA 31 Progress Report 08/01/96, European Gas Turbines, Lincoln, UK, January 1996.
24. Wanhill, R.J.H., Boogers, J.A.M. and Kolkman, H.J., Completing NLR contributions to the IEPG TA 31 programme. Part II: Crack growth testing on CT specimens, NLR Contract Report CR 97035 L, National Aerospace Laboratory NLR, Amsterdam, The Netherlands, February 1997.
25. Affeldt, E., LCF test results of notched specimens for disk rim simulation, Technical Note MTUM-N94EFM-0024, Motoren- und Turbinenunion (MTU), Munich, Germany, November 1994.
26. Wanhill, R.J.H., Hattenberg, T. and ten Hoeve, H.-J., Fractographic examination of three EGT RIM specimens, NLR Contract Report CR 96451 C, National Aerospace Laboratory NLR, Amsterdam, The Netherlands, July 1996.
27. Herbel, H.-M., Amstutz, A., Dankert, M. and Seeger, T., Fracture mechanics analysis of notched specimens under tension and bending loading, Report FI-111/1993, Technische Hochschule Darmstadt, Darmstadt, Germany, May 1993.
28. Wanhill, R.J.H. and Boogers, J.A.M., Completing NLR contributions to the IEPG TA 31 programme. Part I: low cycle fatigue testing, NLR Contract Report CR 97035 L, National Aerospace Laboratory NLR, Amsterdam, The Netherlands, January 1997.
29. Hughes, M., Engineering specimen life prediction and comparisons with test results, Handout for the IEPG TA 31 20th Working Group Meeting, European Gas Turbines, Lincoln, UK, June 1996.
30. Wanhill, R.J.H., Boogers, J.A.M. and Kolkman, H.J., Completing NLR contributions to the IEPG TA 31 programme. Part III: crack growth testing on RIM specimens, NLR Contract Report CR 97035 L, National Aerospace Laboratory NLR, Amsterdam, The Netherlands, February 1997.
31. Wanhill, R.J.H. and Boogers, J.A.M., Completing NLR contributions to the IEPG TA 31 programme. Part IV: crack growth testing on CC specimens, NLR Contract Report CR 97035 L, National Aerospace Laboratory NLR, Amsterdam, The Netherlands, March 1997.
32. Wanhill, R.J.H., Fractographic examination of three IABG LCF specimens, NLR Contract Report CR 97083 L, National Aerospace Laboratory NLR, Amsterdam, The Netherlands, February 1997.
33. Newman, Jr., J.C, and Raju, I.S., Stress-intensity factor equations for cracks in three-dimensional finite bodies subjected to tension and bending loads, NASA Technical Memorandum 85793, National Aeronautics and Space Administration, Langley Research Center, Hampton, USA, April 1984.

34. Mom, A.J.A., Evans, W.J. and ten Have, A.A., TURBISTAN, a standard load sequence for aircraft engine discs, AGARD Conference Proceedings No. 393, Damage Tolerance Concepts for Critical Engine Components, Advisory Group for Aerospace Research and Development, pp. 20-1 – 20-11, Neuilly-sur-Seine, France, October 1985.
35. Pineau, A., High temperature fatigue of Ni-base superalloys: microstructural and environmental effects, Engineering Against Fatigue, A.A. Balkema, pp. 557-565, Rotterdam, The Netherlands, 1999.

Table 1 Heat treatment, mechanical properties and grain size of the IN718 forged pancakes [2]

- Annealing : 955 °C for 1 hour, air cool
- Ageing : 720 °C for 8 hours, furnace cool to 620 °C; 620°C for 8 hours, air cool

0.2 % σ_y (MPa)		σ_{TS} (MPa)		ELONGATION (%)	
R.T	600 °C	R.T.	600 °C	R.T.	600 °C
1195	1030	1440	1230	18	17

- ASTM grain size: 8 or finer, i.e. nominal grain diameter ≤ 22 μm

Table 2 The test programme

- **Dwell cracking: 600°C, CT specimens, test house NLR**

Test type	Load history	P_{dwell} (kN)	P_{max} (kN)
dwell	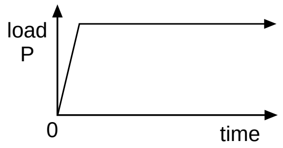	6 7 8 (2x) 10 (3x)	6 7 8 (2x) 10 (3x)
dwell + peak loads and underloads	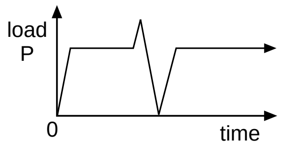	7 8	10 10
	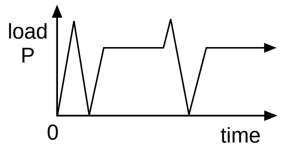	7	10

- **Fatigue crack growth + dwells: 600°C, major cycle R=0·1, marker cycle R=0·8**

Major cycle	Specimen type and test house	Marker cycle (sinewave)	σ_{max} (MPa)	Major cycles to failure	Remarks
2 Hz, sinewave	CT/NLR RIM/EGT	5 Hz	700	60,031	multiple initiation, one notch
0·25 Hz, trapezoidal	CT/NLR RIM/EGT	5 Hz	750	29,259	single initiation
120s dwell, trapezoidal	CT/NLR RIM/EGT	5 Hz	750	28,584	multiple initiation, one notch

- **Flight-by-flight loading: HOT TURBISTAN, 600°C**

Specimen type and test house	σ_{max} (MPa)	ε_{max} (%)	Flights to faillure	Remarks
LCF/IABG		1·05 1·2 1·5	3000 800 405	Strain-controlled LCF tests
CC/NLR	600 650			
RIM/NLR	600 700 750			Crack starters, one per notch at diametrically opposite corners, 0·2 x 0·2 mm

C911-01N

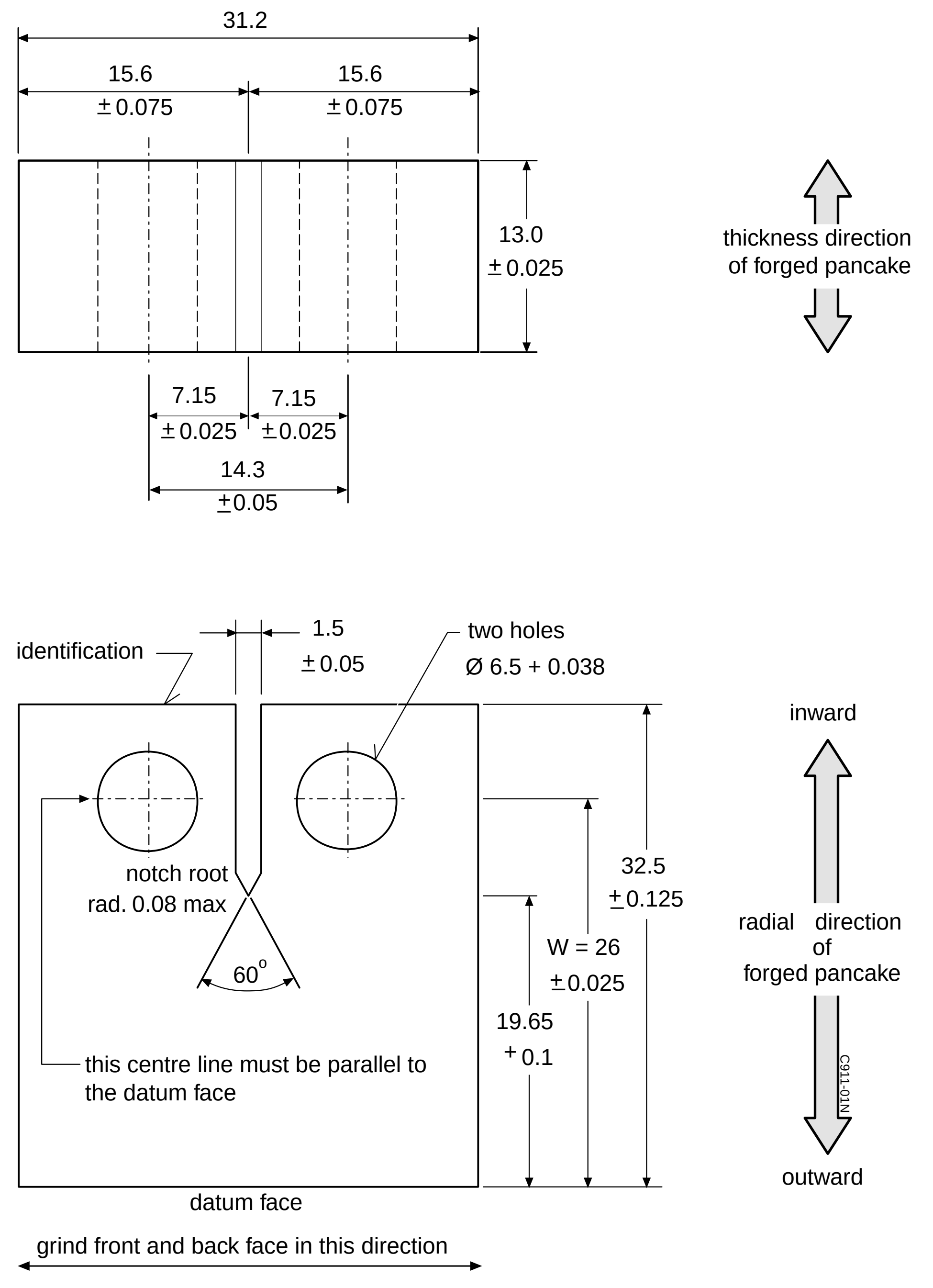

Fig. 1 Compact tension (CT) specimen configuration used for crack growth testing: dimensions in mm

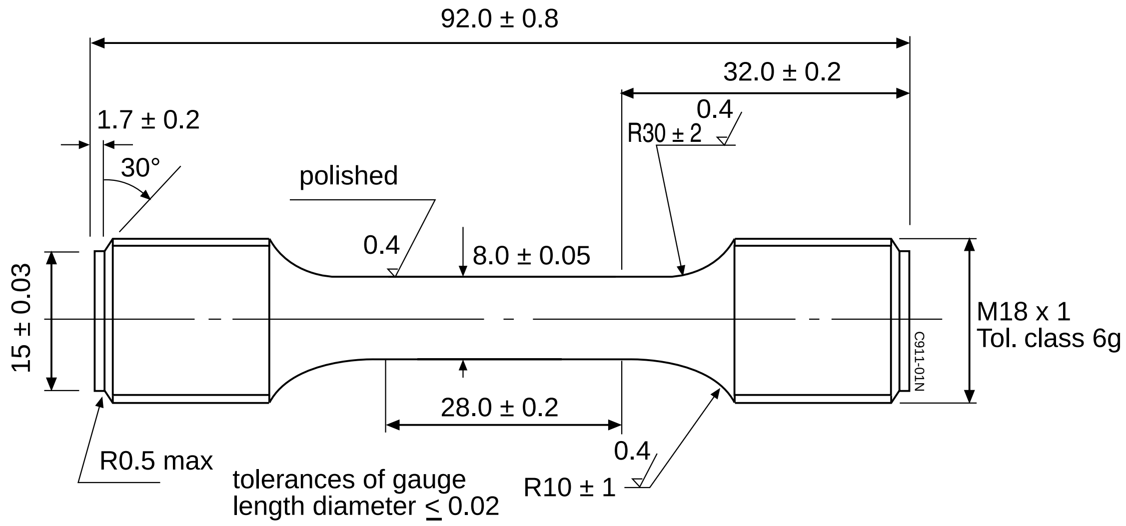

Fig. 2 Low cycle fatigue (LCF) specimen configuration: dimensions in mm

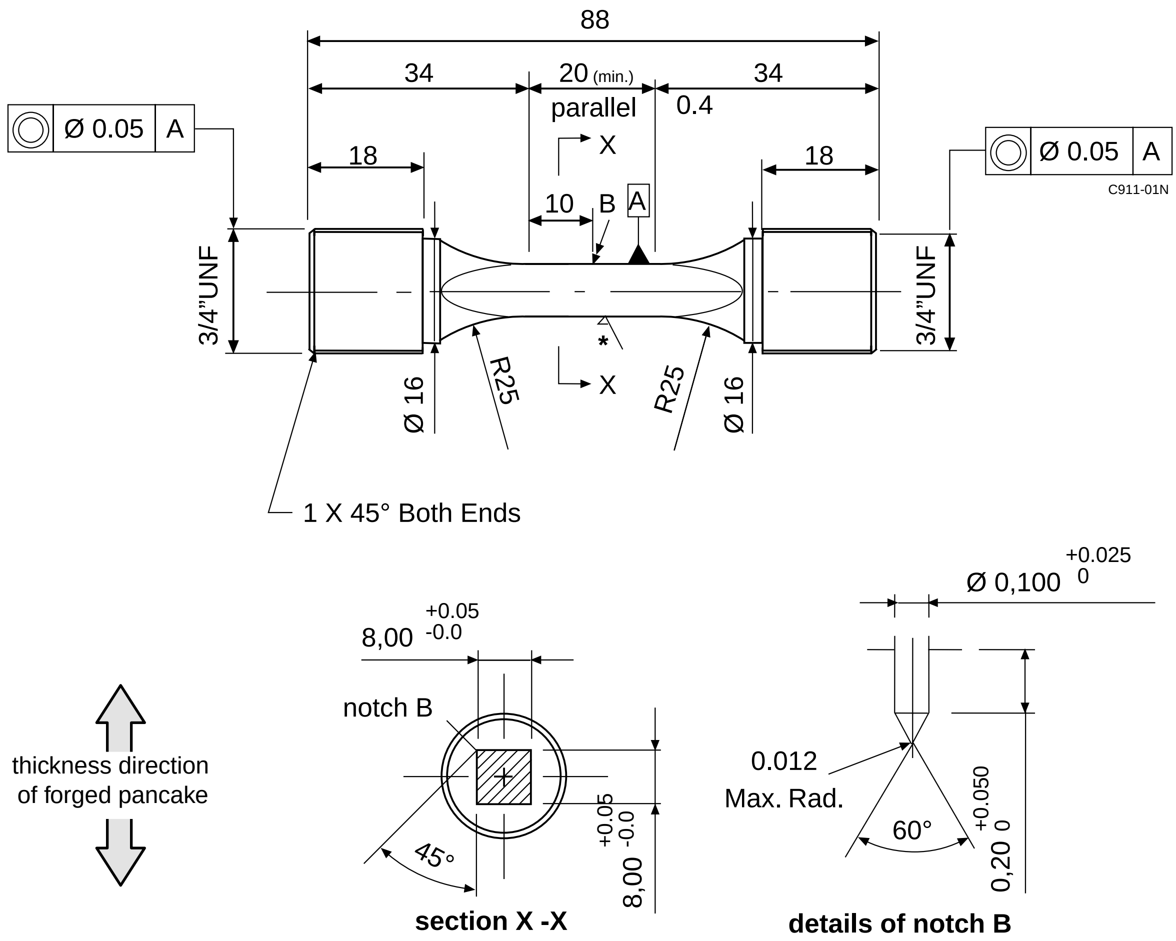

Fig. 3 Corner crack (CC) specimen configuration used for crack growth testing: dimensions in mm

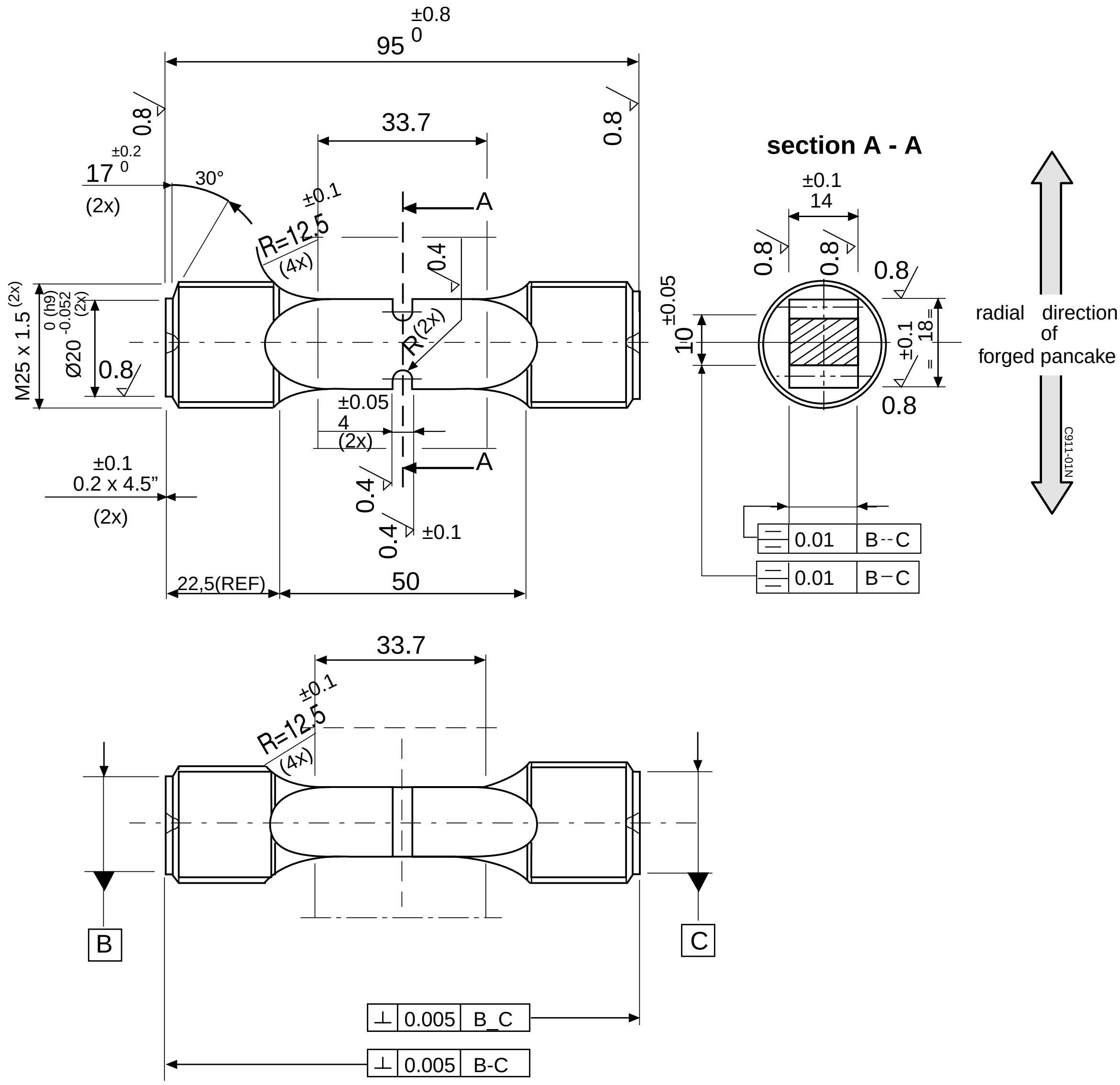

Fig. 4 Engineering rim (RIM) specimen configuration: dimensions in mm, notch surfaces broached or milled, followed by grinding and hand polishing down to 1 μm diamond paste grade [3]

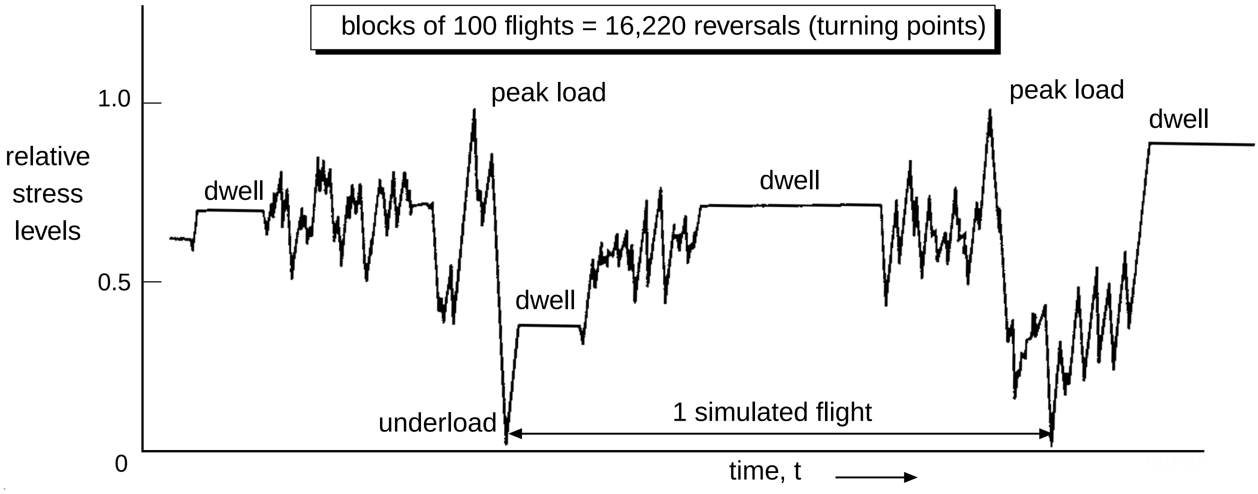

Fig. 5 Typical segment of the turbine disc generic load history HOT TURBISTAN [5]

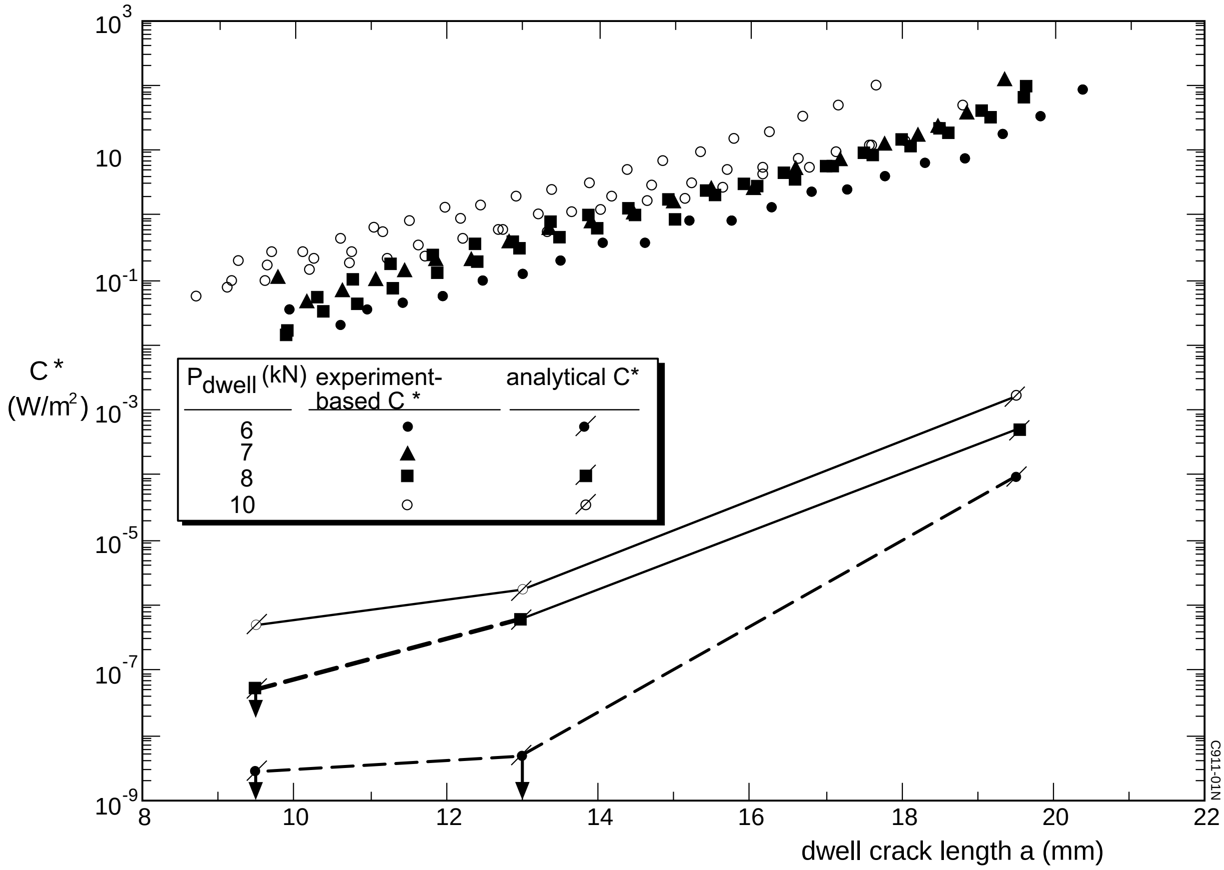

Fig. 6 Experimental and analytical C* for CT specimen dwell cracking at 600°C

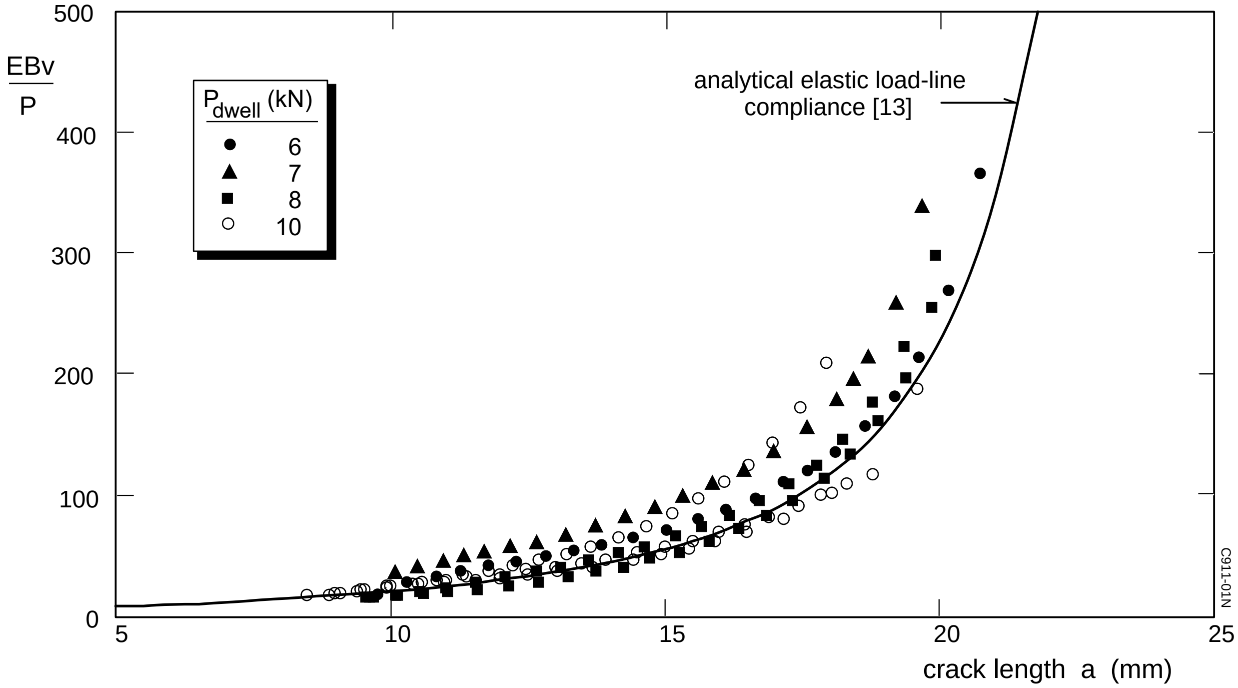

Fig. 7 Comparison of experimental and analytical load-line compliances for the dwell crack growth CT specimens

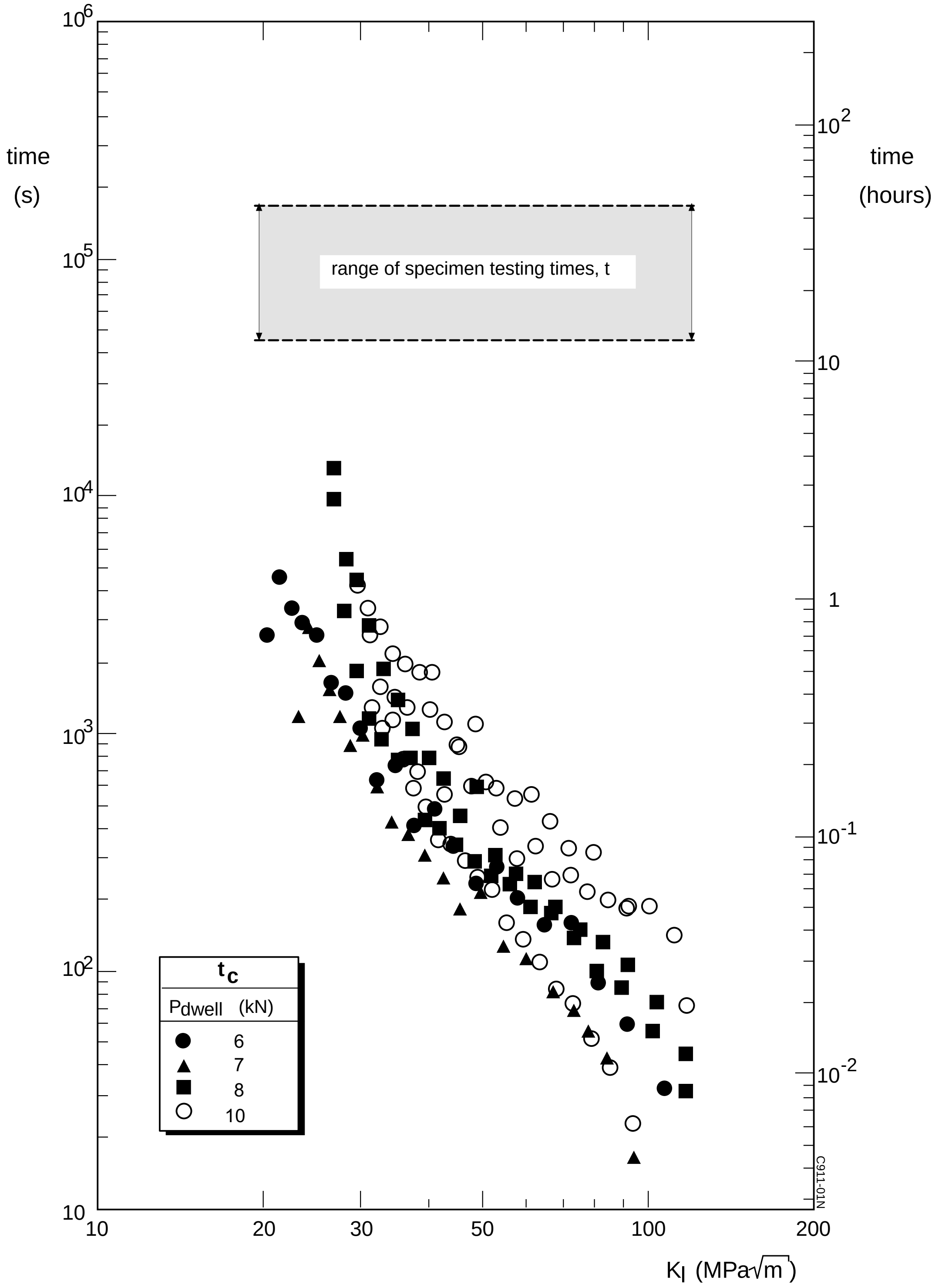

Fig. 8 Comparison of dwell crack growth CT specimen lives with the characteristic times, t_c , calculated with C* values derived by the method of Kumar et al [10]

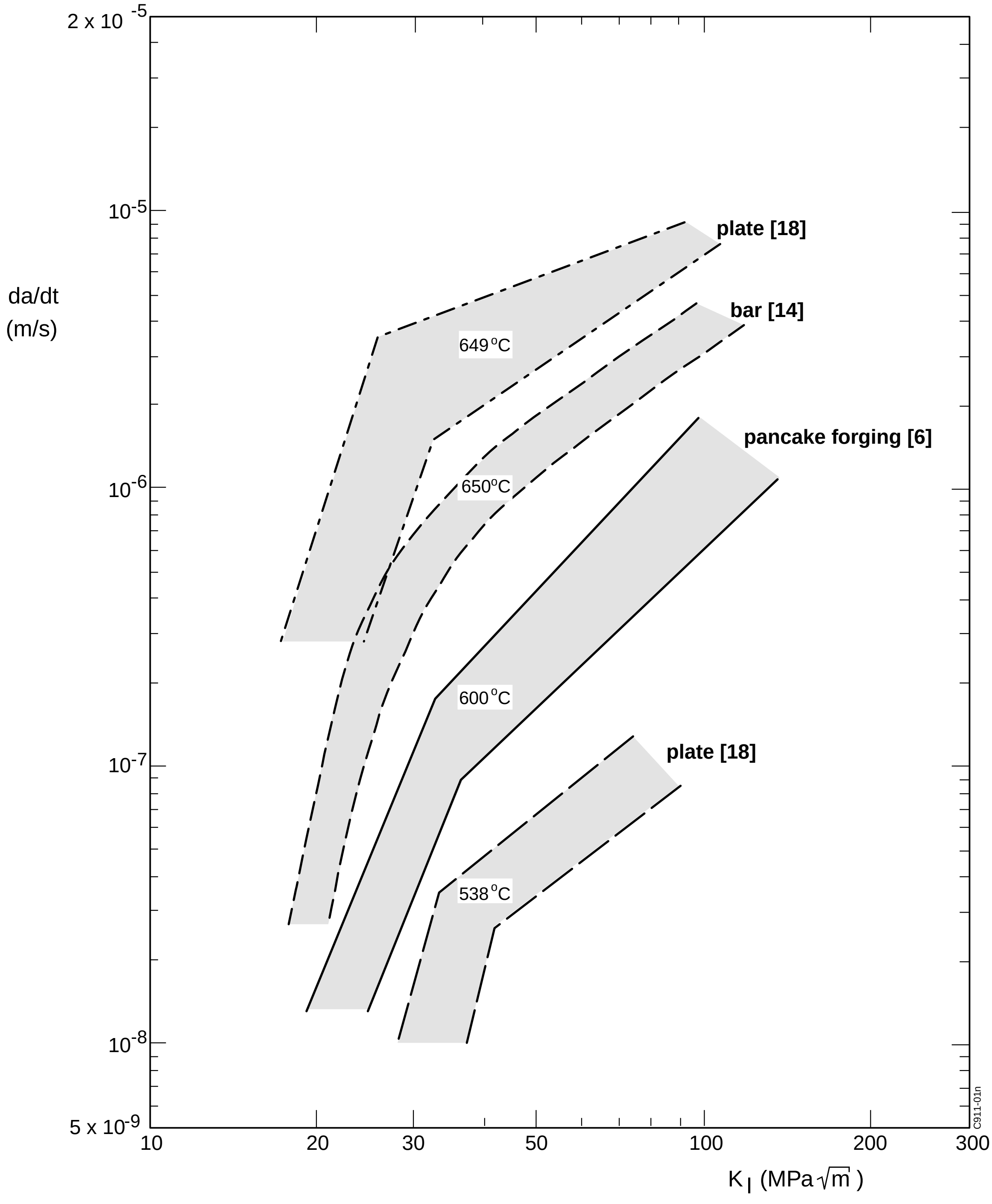

Fig. 9 IN718 dwell crack growth rates versus K_I [6]

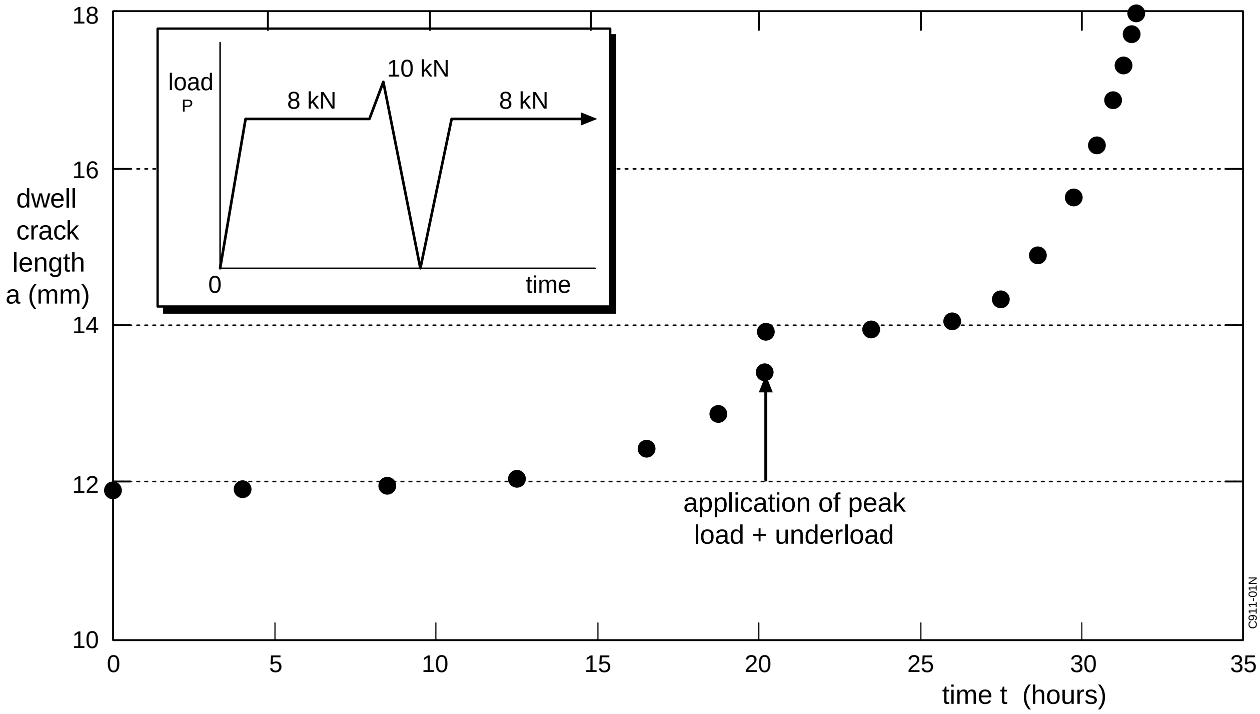

Fig. 10 Example of suppression of dwell cracking by a peak load, Pmax/Pdwell= 1·25, for IN718 at 600°C [6]

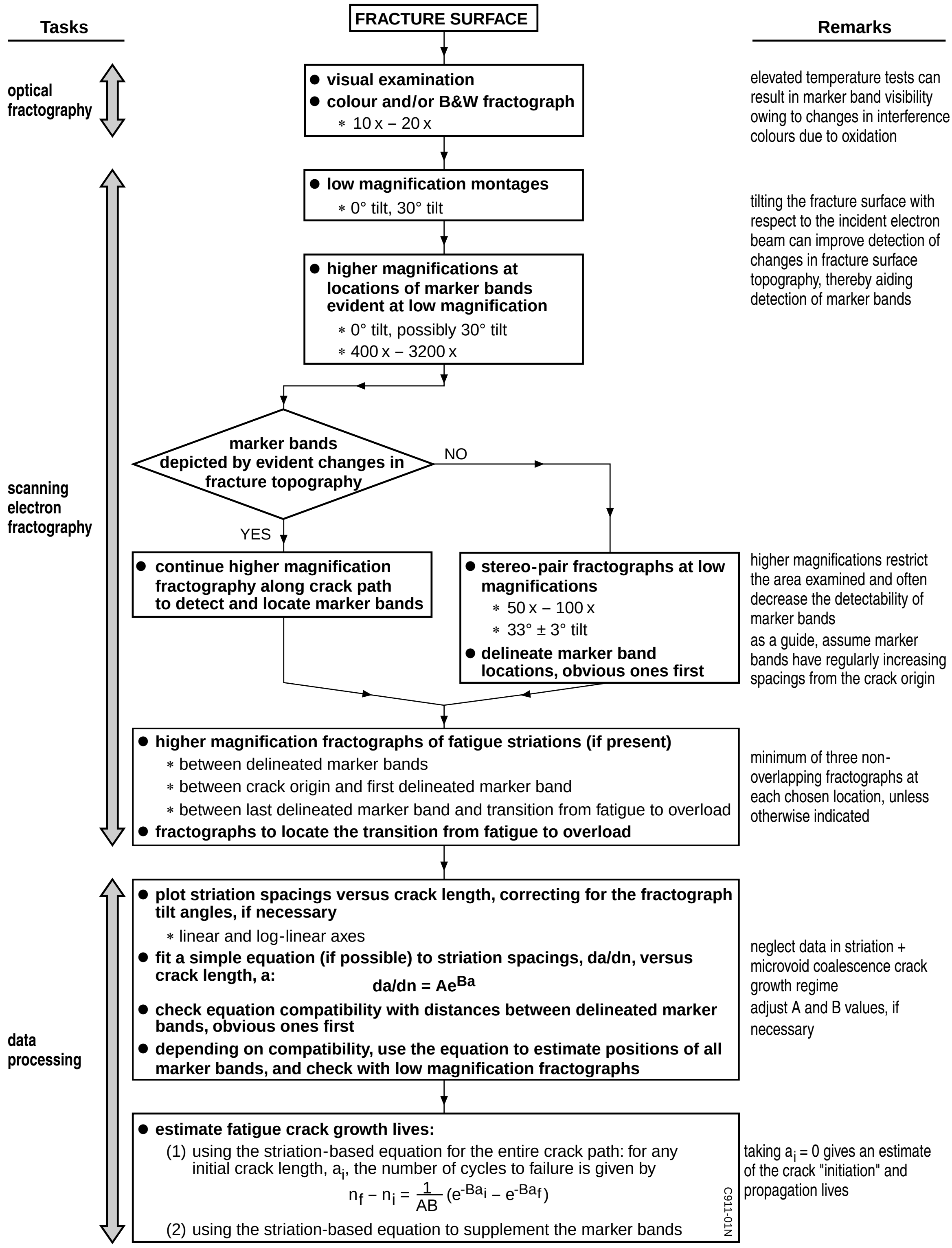

Fig. 11 Fractography-based method of estimating fatigue crack "initiation" and growth lives and fatigue crack growth rates for RIM specimens tested under constant amplitude loading interspersed with marker band loading [26]

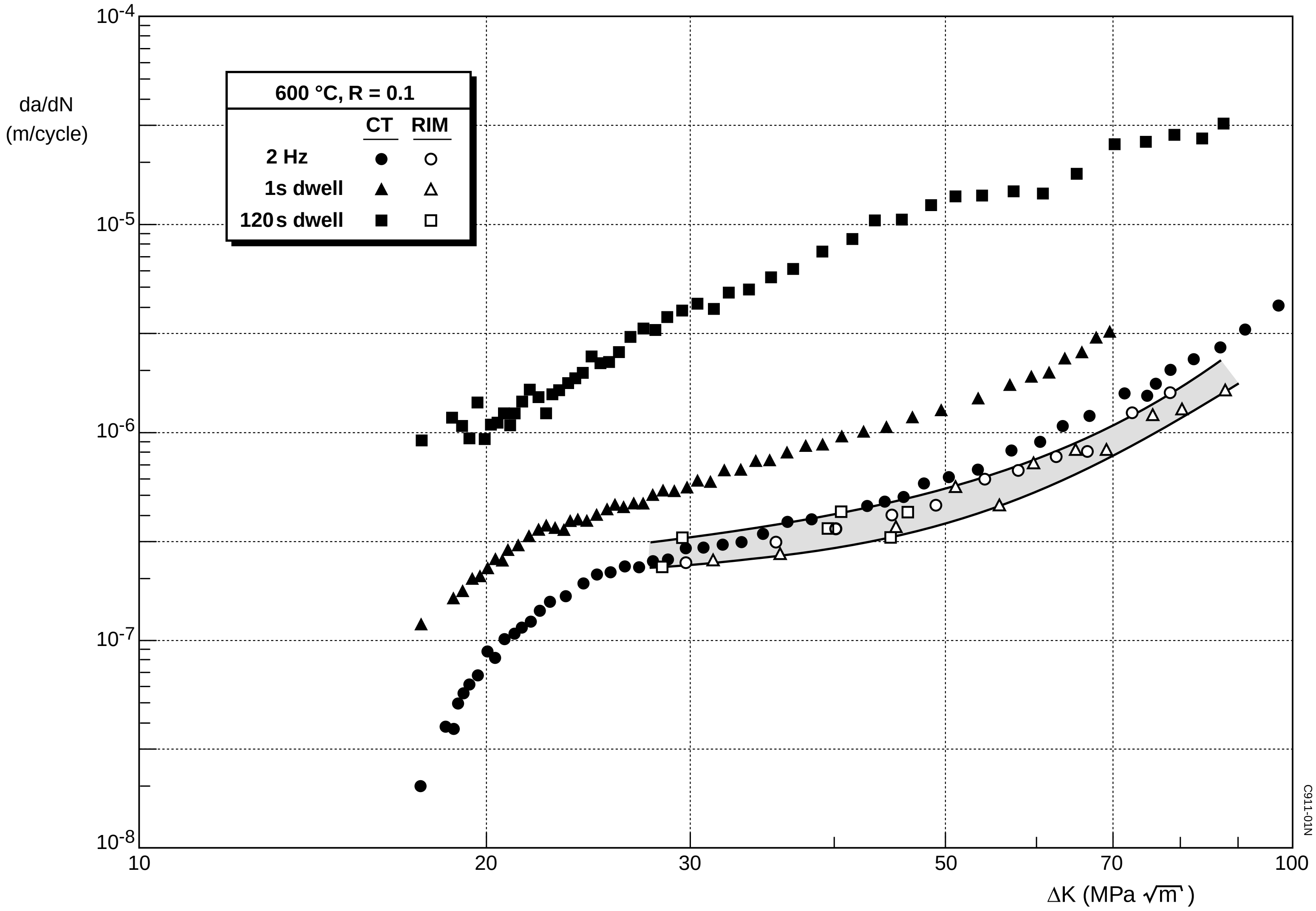

Fig. 12 Crack growth rates (fatigue crack growth with and without dwells) for CT and RIM specimens [26]. The CT data are fully reported in Ref. [24]

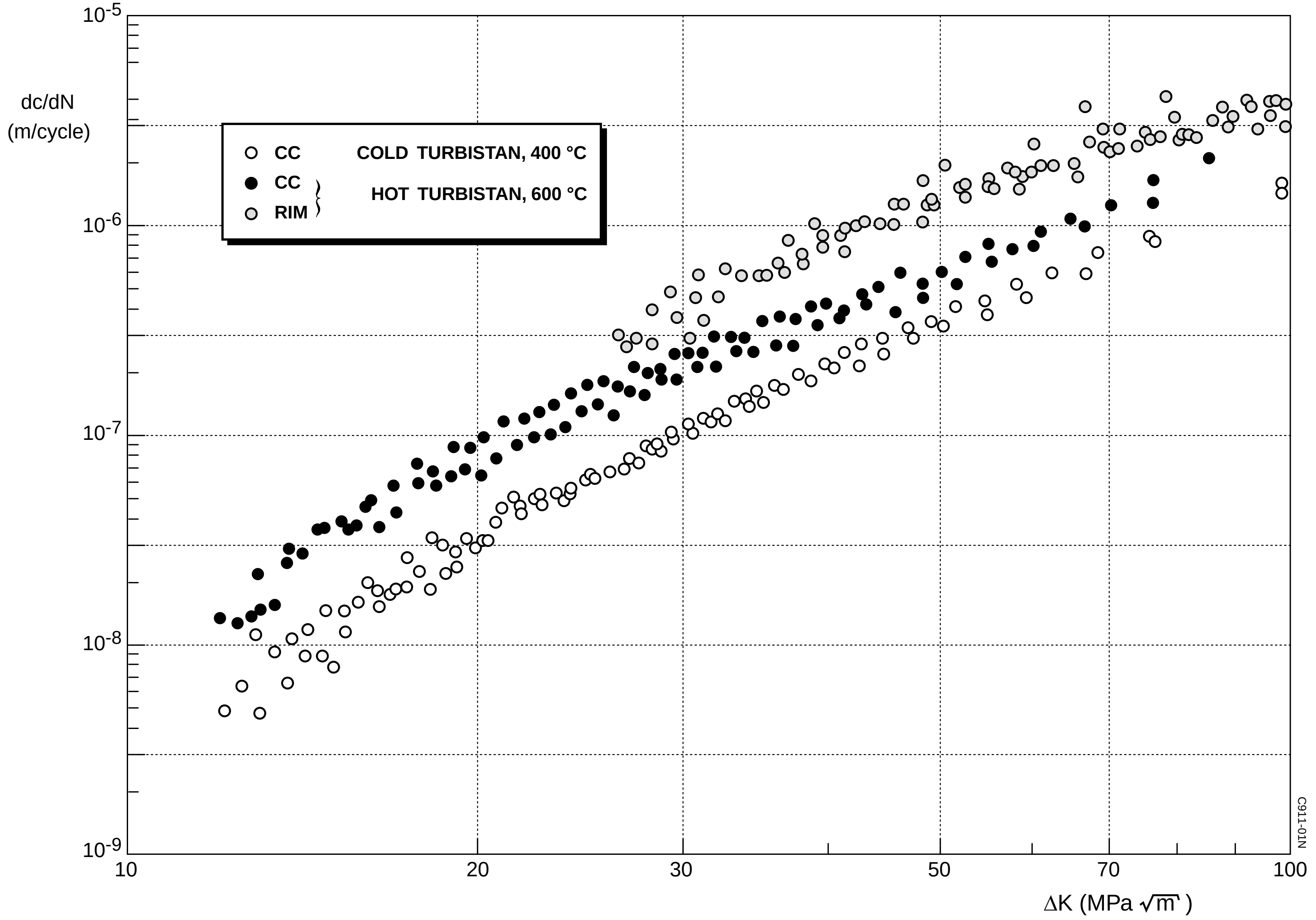

Fig. 13 Flight-by-flight loading crack growth rates for CC and RIM specimens. The tests are reported in Refs. [30,31]. N.B.: for the CC specimens c = a; for the RIM specimens c = notch surface crack length ≈1.33a